

Fluorescence from doubly driven four-level atoms - A density Matrix approach.

ANDAL NARAYANAN, R.SRINIVASAN, ASHOK VUDAYAGIRI, UDAY KUMAR KHAN AND
HEMA RAMACHANDRAN

Raman Research Institute, Sadashivnagar, Bangalore, INDIA 560 080

Abstract. – The unusually narrow features in the fluorescence from ^{85}Rb driven by the cooling and repumper laser fields, reported in [1], are explained on the basis of a four-level density matrix calculation. Quantum effects alter the efficiency of atom transfer by the probe (repumper) laser to the levels connected by the pump (cooling) laser. This, combined with the double resonance condition [1], leads to velocity selection from co-propagating and counter propagating pump and probe beams resulting in narrow fluorescence peaks from a thermal gas at room temperature.

Introduction. – Multilevel atoms, under the action of multiple fields, display a variety of phenomena brought about by the ac Stark splitting of electronic levels and by interference due to induced coherences. These manifest themselves as splitting of peaks, inhibition of absorption or emission, narrow windows of transparency, etc. Theoretical work on this front have considered Λ , V and ladder type of three level systems [2]. The presence of additional levels increases multifold the possibilities of interference phenomena that exist. The nested Λ and the N systems have been examined to some extent [3]. In this paper we examine an "inverted N" system using the density matrix formalism. Recent experimental observations in ^{85}Rb [1] have prompted the study of this four-level system under the action of two fields.

Experiment. – The experiment in [1] consisted of driving a collection of ^{85}Rb atoms with two fields- a strong "cooling" field and a weak "repumper" field. One of the lasers, the cooling (pump) laser was held at a fixed detuning δ_c from the conventional cooling transition $(^1) (5S_{1/2}, F = 3 \rightarrow 5P_{3/2}, F' = 4')$ and the repumper (probe) laser was scanned with its detuning (δ_r) from $5S_{1/2}, F = 2 \rightarrow 5P_{3/2}, F' = 3'$ level varying over the entire manifold, $F=2 \rightarrow F'=1', 2', 3'$ (See Fig. 1) $(^2)$. Narrow fluorescence peaks were observed at definite δ_r for a given δ_c . While one would expect a broad fluorescence, with the width indicative of the temperature of the gas, the experiment showed fluorescence peaks just 30MHz in width, much smaller than their Doppler width of 500MHz. This was explained on the basis of a double resonance model which maximised fluorescence whenever the atom found both the cooling and repumping lasers on resonance with their respective transitions. A simple analytical treatment based on the above model showed that atom transfer efficiency by the repumper laser to the

⁽¹⁾The cooling and repumper beams are used in the sense as defined in [1].

⁽²⁾Hyperfine levels of $5S_{1/2}$ are denoted unprimed while that of $5P_{3/2}$ are denoted primed.

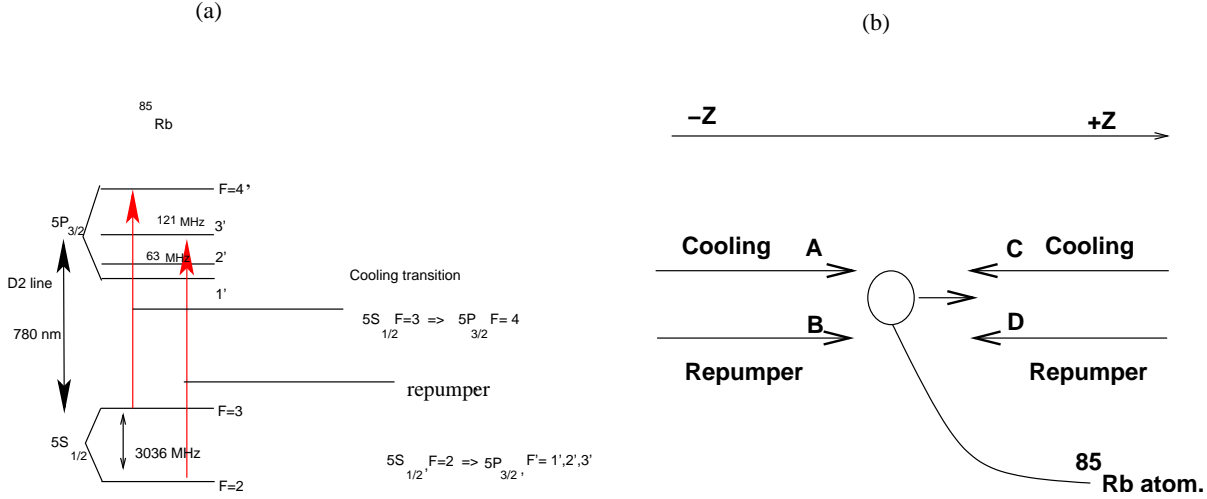


Fig. 1 – (a): Energy level diagram of ^{85}Rb . (b): A one dimensional configuration (along \mathbf{Z}) of the cooling and repumper beams with the ^{85}Rb atom taken move along $+z$ direction

levels connected by the cooling laser was maximised under the double resonance condition and gave rise to narrow fluorescence peaks.

In this paper, we present a rigorous treatment of the same problem using a four level density matrix formalism. Our treatment differs from the earlier studies of four-level density matrix [4] in that (a) it considers an inverted N system and (b) it takes into account the motion of the atoms in co- and counter-propagating geometries with respect to the cooling and repumper beams.

Four Level Density Matrix. – The four levels under consideration are: the two ground hyperfine levels $F=2,3$ and the two excited levels $F'=3',4'$. For simplicity, we have considered an one dimensional situation where the two driving fields are in the $\pm z$ direction and the atom is moving along the z direction with a velocity \vec{v} . The detuning of the cooling laser taking the Doppler effect into account is $\Delta_c = \delta_c - \vec{k}_c \cdot \vec{v}$ and the repumper laser's detuning is $\Delta_r = \delta_r - \vec{k}_r \cdot \vec{v}$ where, δ_c and δ_r are the detunings of the laser in the laboratory frame. The total Hamiltonian for the system consisting of the atom and the light fields is written in the interaction picture as

$$H = H_0 + H_I \quad (1)$$

where H_0 is the Hamiltonian for the bare atom and H_I is the atom-light interaction Hamiltonian. They are given as

$$H_0 = \hbar\omega_2 |2\rangle\langle 2| + \hbar\omega_3 |3\rangle\langle 3| + \hbar\omega_{3'} |3'\rangle\langle 3'| + \hbar\omega_{4'} |4'\rangle\langle 4'|$$

and

$$H_I = -\frac{\hbar}{2} [\Omega_{34'} |3\rangle\langle 4'| \exp(-i\omega_{LC}t) + \Omega_{33'} |3\rangle\langle 3'| \exp(-i\omega_{LC}t) + \Omega_{23'} \exp(-i\omega_{LR}t) |2\rangle\langle 3'| + H.C]$$

Here the $\hbar\omega_i$ represent the energies of the levels as represented in Figure 1, with $\hbar\omega_2$ taken as zero, ω_{LC} and ω_{LR} the frequencies of the cooling and repumper laser beams and $\Omega_{ij'}$ is the Rabi frequency connecting the levels i and j' . The total Hamiltonian can be written in

matrix form as follows

$$H = \begin{vmatrix} \hbar\omega_2 & 0 & -\frac{\hbar}{2}\Omega_{23'}e^{(-i\omega_{LR}t)} & 0 \\ 0 & \hbar\omega_3 & -\frac{\hbar}{2}\Omega_{33'}e^{(-i\omega_{LC}t)} & -\frac{\hbar}{2}\Omega_{34'}e^{(-i\omega_{LC}t)} \\ -\frac{\hbar}{2}\Omega_{23'}e^{(i\omega_{LR}t)} & -\frac{\hbar}{2}\Omega_{33'}e^{(i\omega_{LC}t)} & \hbar\omega_{3'} & 0 \\ 0 & -\frac{\hbar}{2}\Omega_{34'}e^{(i\omega_{LC}t)} & 0 & \hbar\omega_{4'} \end{vmatrix}$$

where the rows and columns correspond to levels 2, 3, 3', 4' in sequence. The dynamics of the system described by this Hamiltonian can be studied using the density matrix $\rho = \sum \rho_{ij}|i\rangle\langle j|$. The time evolution of the density matrix ρ is given by the Liouville equation

$$\frac{d\rho}{dt} = -\frac{i}{\hbar}[H, \rho] - \frac{1}{2}\{\Gamma, \rho\} \quad (2)$$

with

$$\Gamma_{ij} = 2\gamma_{i' \rightarrow j}\delta_{ij'} \quad (3)$$

where $\gamma_{i' \rightarrow j}$ being the spontaneous decay rate from the j^{th} level to the i'^{th} level. ⁽³⁾ The rate equations of the four levels for an atom moving with a velocity v are derived under the rotating wave approximation. They are

$$\frac{d\rho_{11}}{dt} = -\frac{i}{2}[\Omega_{23'}\rho_{31} - \Omega_{23'}^*\rho_{13}] + 2\gamma_{3'2}\rho_{33'} \quad (4)$$

$$\frac{d\rho_{12}}{dt} = -i(\Delta_{c3'} - \Delta_r) - \frac{i}{2}[\Omega_{23'}\rho_{32} - \Omega_{33'}^*\rho_{13} - \Omega_{34'}^*\rho_{14}] \quad (5)$$

$$\frac{d\rho_{13}}{dt} = (i(\Delta_r) - (\gamma_{3'2} + \gamma_{3'3}))\rho_{13} - \frac{i}{2}[\Omega_{23'}\rho_{33} - \Omega_{23'}^*\rho_{11} - \Omega_{33'}^*\rho_{12}] \quad (6)$$

$$\frac{d\rho_{14}}{dt} = -i[(\Delta_{c3'} - \Delta_c - \Delta_r) - \gamma_{4'3}]\rho_{14} - \frac{i}{2}[\Omega_{23'}\rho_{34'} - \Omega_{34'}\rho_{12}] \quad (7)$$

$$\frac{d\rho_{21}}{dt} = i(\Delta_{c3'} - \Delta_r)\rho_{21} - \frac{i}{2}[\Omega_{33'}\rho_{31} + \Omega_{34'}\rho_{41} - \Omega_{23'}\rho_{23}] \quad (8)$$

$$\frac{d\rho_{22}}{dt} = -\frac{i}{2}[\Omega_{33'}\rho_{32} + \Omega_{34'}\rho_{42} - \Omega_{33'}\rho_{23} - \Omega_{34'}\rho_{24}] + 2\gamma_{3'3}\rho_{33} + 2\gamma_{4'3}\rho_{44} \quad (9)$$

$$\frac{d\rho_{23}}{dt} = (i\Delta_{c3'} - (\gamma_{3'2} + \gamma_{3'3}))\rho_{23} - \frac{i}{2}[\Omega_{33'}\rho_{33} + \Omega_{34'}\rho_{43} - \Omega_{23'}\rho_{21} - \Omega_{33'}\rho_{22}] \quad (10)$$

$$\frac{d\rho_{24}}{dt} = (i\Delta_c - \gamma_{4'3})\rho_{24} - \frac{i}{2}[\Omega_{33'}\rho_{34} + \Omega_{34'}\rho_{44} - \Omega_{34'}\rho_{22}] \quad (11)$$

$$\frac{d\rho_{31}}{dt} = (-i\Delta_r - (\gamma_{3'2} + \gamma_{3'3}))\rho_{31} - \frac{i}{2}[\Omega_{23'}^*\rho_{11} + \Omega_{33'}^*\rho_{21} - \Omega_{23'}^*\rho_{33}] \quad (12)$$

$$\frac{d\rho_{32}}{dt} = (-i\Delta_{c3'} - (\gamma_{3'2} + \gamma_{3'3}))\rho_{32} - \frac{i}{2}[\Omega_{33'}^*\rho_{22} - \Omega_{33'}^*\rho_{33} - \Omega_{34'}\rho_{34}] \quad (13)$$

$$\frac{d\rho_{33}}{dt} = -2(\gamma_{3'2} + \gamma_{3'3})\rho_{33} - \frac{i}{2}[\Omega_{23'}\rho_{13} + \Omega_{33'}\rho_{23} - \Omega_{23'}\rho_{31}] \quad (14)$$

$$\frac{d\rho_{34}}{dt} = [(i\Delta_{c3'} - \Delta_c) - (\gamma_{3'2} + \gamma_{3'3} + \gamma_{4'3})]\rho_{34} - \frac{i}{2}[\Omega_{23'}^*\rho_{14} + \Omega_{33'}^*\rho_{24} - \Omega_{34'}\rho_{32}] \quad (15)$$

$$\frac{d\rho_{41}}{dt} = [(i\Delta_{c3'} - \Delta_c - \Delta_r) - \gamma_{4'3}]\rho_{41} - \frac{i}{2}[\Omega_{34'}^*\rho_{21} - \Omega_{23'}^*\rho_{43}] \quad (16)$$

$$\frac{d\rho_{42}}{dt} = [(i\Delta_c - \gamma_{4'3})]\rho_{42} - \frac{i}{2}[\Omega_{34'}^*\rho_{22} - \Omega_{33'}^*\rho_{43} - \Omega_{34'}^*\rho_{44}] \quad (17)$$

⁽³⁾where $\Gamma_{ij'}$ is the decay rate of the level j to the level i' . This is however a diagonal matrix

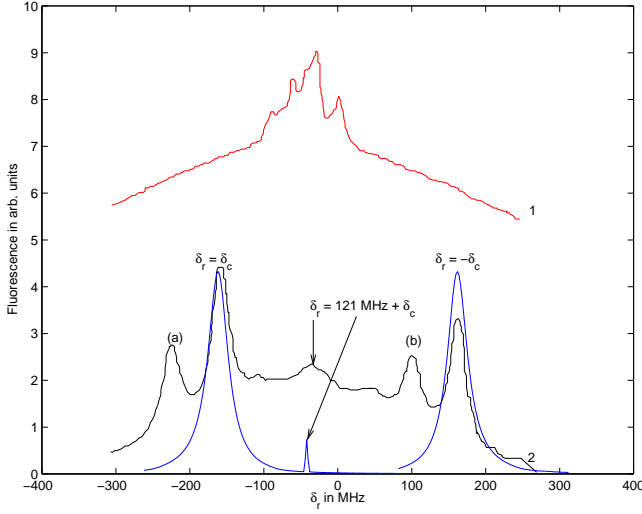


Fig. 2 – Trace 1 shows the saturation absorption spectrum of the repumper. Trace 2 shows the experimental curve (black) and the corresponding theoretical curve (blue). See text for explanation on the (a) and (b) peaks in the figure.

$$\frac{d\rho_{43}}{dt} = [-i(\Delta_{c3'} - \Delta_c) - (\gamma_{3'2} + \gamma_{3'3} + \gamma_{4'3})]\rho_{43} - \frac{i}{2}[\Omega_{34'}\rho_{23} - \Omega_{33'}\rho_{42} - \Omega_{34'}^*\rho_{23'}\rho_{41}] \quad (18)$$

$$\frac{d\rho_{44}}{dt} = -\frac{i}{2}[\Omega_{34'}^*\rho_{24} - \Omega_{34'}\rho_{42} - 2\gamma_{4'3}\rho_{44}] \quad (19)$$

For each velocity \vec{v} steady state values of ρ_{ij} are obtained by numerically solving the above rate equations for various values of δ_c and δ_r , subject to the constraint $\sum_{i=1}^4 \rho_{ii} = 1$. Thus for an atom with a velocity \vec{v} we obtain the population of each level and coherence between various levels for different values of δ_r and δ_c . The fluorescence emitted by atoms with a velocity \vec{v} is given by

$$\text{Fluorescence}(\Delta_c, \Delta_r) = \Gamma_{4'3}\rho_{4'4'} + \Gamma_{3'3}\rho_{33'} + \Gamma_{3'2}\rho_{3'3'} \quad (20)$$

As the detector collects fluorescence from atoms which are in thermal motion, we take the average of each ρ_{ij} value over the range of velocities, weighted by the one dimensional Maxwellian velocity distribution. The fluorescence calculated as above as a function of δ_r and the corresponding experimental data are given in Fig. 2 for a cooling laser detuning $\delta_c = -162$ MHz. A general agreement between the results of our calculation and that of the experiment is seen.

⁽⁴⁾ The individual features will be discussed in detail below.

Discussion. – Consider a situation shown in Fig. 1b, when the cooling and repumping beams are both along $\pm z$ directions. Initially let us consider the atoms to be at rest. For a given detuning δ_c of the cooling (pump) laser, we should get fluorescence peaks corresponding to the Autler-Townes (AT) dressed states of $F' = 3'$ at the probe (repumper) detunings [5]

$$\delta_{r\pm} = \frac{\delta_{c3'}}{2} \pm \sqrt{(\delta_{c3'}^2 + \Omega^2)}/2 \quad (21)$$

⁽⁴⁾Peaks (a) and (b) seen in the experiment arise due to the transitions from $F' = 2'$ level which has not been included in our density matrix

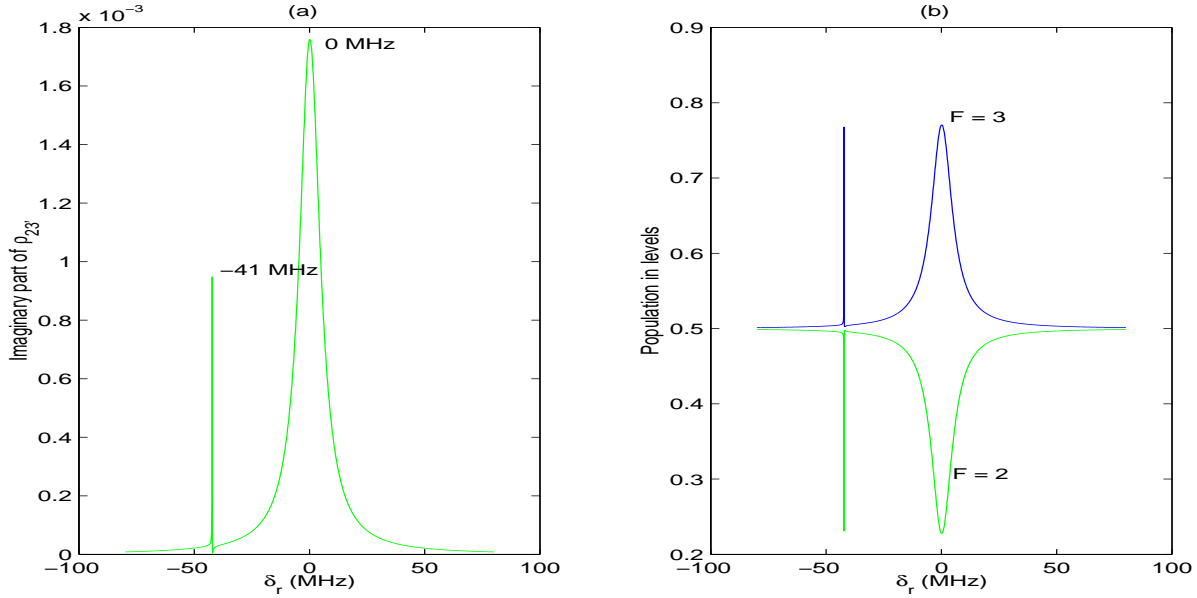


Fig. 3 – The imaginary part of $\rho_{23'}$ vs the positions of the probe absorption δ_r showing that absorption of the repumper (probe) light due to Autler -Townes splitting of the level $F' = 3'$ occurs at the detunings 0MHz and -41MHz . (b) ρ_{33} (blue) and ρ_{22} (green) as functions of δ_r .

Here $\delta_{c3'} = 2\pi * 121\text{MHz} + \delta_c$ denotes the detuning of the cooling laser from $3 \rightarrow 3'$ transition, 121 MHz being the level spacing between $F' = 3'$ and $4'$ levels and Ω its Rabi frequency. For the specific case shown in figure 2, for a cooling laser detuning $\delta_c = -162\text{MHz}$ and for small Ω , the Autler-Townes peak positions for these zero velocity atoms are $\delta_{r\pm} \approx 0, -41\text{MHz}$. This is confirmed from our density matrix calculations. At these detunings of the probe its absorption is maximised and repumping most efficient as seen from Figs. 3(a) and 3(b) which give $\rho_{23'}$, ρ_{33} and ρ_{22} as functions of δ_r .

Consider now an atom in motion with a velocity $+v$, along the $+z$ direction. If $\delta_c < 0$ this atom predominantly absorbs from the cooling beam coming towards it (C). Since the repumper laser is scanned, depending on the sign of δ_r the atom absorbs either from B or from D. So for a given δ_c , altogether we get four peaks, a Autler-Townes pair each shifted due to the Doppler effect, depending upon whether absorption takes place from the repumper beam B or from repumper beam D. The same holds for $\delta_c > 0$ for atoms with velocity $-v$.

The AT doublet positions as given in equation (21) when applied to atoms in motion and, for small Ω and $\delta_c < 0$ are

$$\delta_{r-} - (\pm kv) \approx 0; \quad \delta_{r+} - (\pm kv) \approx \delta_{c3'} - (\pm kv) \quad (22)$$

As the repumper is scanned, maximum transfer of population from $F=2$ to $F=3$ will occur when these conditions are satisfied. Now, as mentioned in [1] and as will be shown shortly, the fluorescence is predominantly from $4' \rightarrow 3$. However, not all atoms in $F=3$ will be in resonance with the cooling laser; only a small velocity class around $v_c = \delta_c/k$ will give rise to fluorescence. This is the mechanism that gives rise to narrow velocity selection from a hot gas. This velocity selection effect is confirmed by our calculations and is shown in Fig. 4 which gives $\rho_{4'4'}$ and $\rho_{3'3'}$ as functions of the velocity of the atom for $\delta_c = \delta_r = -162\text{MHz}$. We

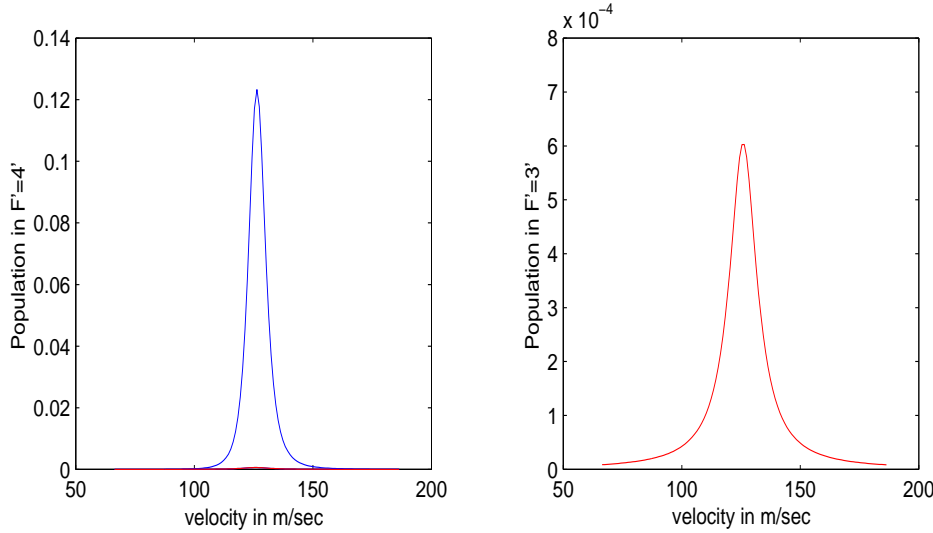


Fig. 4 – Populations in the upper levels $F' = 3$ and $F' = 4'$. The very low population of $F' = 3'$ in (a) is shown magnified in (b).

see that the population in $F'=4'$ ($\rho_{4'4'}$) is two orders more than that in $F'=3'$ ($\rho_{3'3'}$) and it peaks at the critical velocity $v_c = 126 \text{ m/sec}$. Therefore only for velocities around v_c will the fluorescence from $F' = 4'$ be maximised, showing that indeed the double resonance condition selects a narrow velocity class for fluorescence.

The Autler-Townes peak positions, as given by equations (22), with the constraint that double resonance should also be satisfied for maximum fluorescence, require that

$$\delta_{r-} = \delta_c; \quad \delta_{r+} = 121 \text{ MHz} + \delta_c \quad (23)$$

when repumper absorption takes place from D and

$$\delta_{r-} = -\delta_c; \quad \delta_{r+} = 121 \text{ MHz} - \delta_c (v = v_c); \quad \delta_{r+} = 121 \text{ MHz} + \delta_c + 2kv (v \neq v_c) \quad (24)$$

when repumper absorption takes place from B.

The same conditions result for atoms with a velocity $-v$, for $\delta_c > 0$. It has been estimated in [5] that the peak at δ_{r-} is broad and the one at δ_{r+} is narrow. The width of the AT peaks decide the prominence of a fluorescence peak as it decides the number of atoms participating in the fluorescence. Thus for peak positions $\delta_{r-} = \delta_c$ & $-\delta_c$ we expect a large fluorescence whereas for the peak at $\delta_{r+} = 121 \text{ MHz} + \delta_c$ we expect a much smaller fluorescence as is indeed seen from experiment and from our calculations (Fig. 2). As mentioned in [1] this peak is well resolved only at large detunings.

The peak around $\delta_{r+} = 121 \text{ MHz} + \delta_c + 2kv$ is absent both in experiment and in our density matrix calculation. For this case, the repumper absorption takes place from B whereas the cooling is absorbed from C. When the absorption takes place from counter-propagating cooling and repumper beams the velocity class satisfying the double resonance is severely restricted. In fact only for $v = v_c$ will the double resonance condition be satisfied. Atoms with $v \neq v_c$ will see the cooling and repumper to be shifted by different detunings and hence will not contribute to the fluorescence. Thus the peaks resulting from this configuration will not be

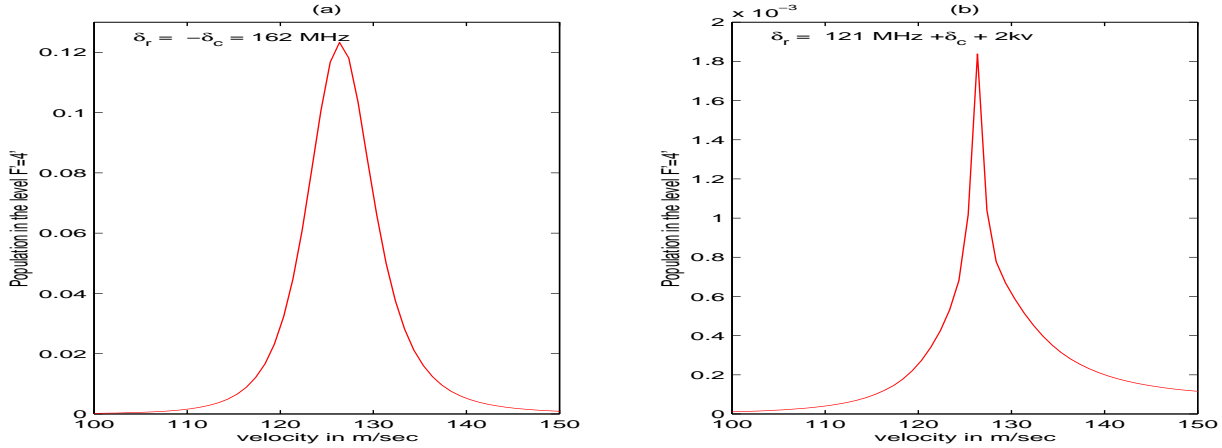


Fig. 5 – Population in the level $F' = 4'$ as a function of the velocity of atoms for the Autler-Townes peaks at (a) $\delta_r = -\delta_c = 162 \text{ MHz}$ (b) $\delta_r = 121 \text{ MHz} + \delta_c + 2kv$.

resolvable as only a very small number of atoms contribute to it. The severely restricted velocity range at resonance resulting in the absence of the peak at $121 \text{ MHz} + \delta_c + 2kv$ is illustrated in Fig. 5b which is obtained from the density matrix calculation. As we see here, only a small number in a very narrow velocity range contribute to population in $F'=4'$ in contrast to the case $\delta_{r-} = -\delta_c$ (Fig. 5a).

The peaks marked (a) and (b) in Figure 2 are the peaks corresponding to the AT levels of $F' = 2'$ at $\delta_{r-} = \delta_c$ & $-\delta_c$ corresponding to absorption from counter and co-propagating repumper beams. Our calculation has not reproduced this peak, as the level $F'=2'$ was not included in the density matrix. Nevertheless the peak positions can be simply calculated from the corresponding peaks for $F'=3'$ by shifting them by -63 MHz . The peak at $\delta_c + 121 \text{ MHz}$ falls at the same δ_{r+} for both $F' = 2'$ and $F' = 3'$.

The theoretically calculated widths of the fluorescence peaks match the experimentally observed narrow width of about 30 MHz . It should be emphasised that this does not arise due to the cooling of atoms in the optical molasses like configuration but due to the velocity selection as discussed above. These fluorescence peaks are experimentally seen to be narrow even for blue detunings of the cooling beam where no cooling occurs and the atoms are at *room temperature*. The corresponding Doppler width is several hundred MHz at this temperature. The additional effects of cooling on these fluorescent peaks in a Doppler free beam geometry will be discussed elsewhere.

Conclusions. – The experimental observations of [1] has been explained using a four-level density matrix formalism. The theory finds that the fluorescence peaks are given rise by the Autler-Townes (AT) doublets of $F' = 3'$ and $F' = 2'$ for atoms around a particular velocity class. The theory gives the three AT peaks of $F' = 3'$ at positions borne out by the experiment. The theory also explains the absence of the fourth peak. The widths and heights of the peaks agree quite well with the experimentally obtained widths and heights.

REFERENCES

- [1] Uday Kumar Khan *et.al to be published*

- [2] Harris, S.E., *Phys. Today*, **50**, 36 and references therein.
Zibrov, A.S. *et.al*, *PRL* **75** (1995),1499.
- [3] de Echaniz, S.R., *et.al Phys. Rev. A* **64** (2001),013812
- [4] Wei C., *et.al Phys. Rev. A* **58** (1998) 2310
- [5] Vemuri G *et.al*, *Phys. Rev. A* **53** (1996), 2842